American Mineralogist, Volume 83, pages 434–443, 1998

Structural mechanisms of solid solution and cation ordering in augite-jadeite pyroxenes: II. A microscopic perspective

TIZIANA BOFFA BALLARAN,[1,*] MICHAEL A. CARPENTER,[2] M. CHIARA DOMENEGHETTI,[3] EKHARD K.H. SALJE,[2] AND VITTORIO TAZZOLI[1]

[1]Dipartimento di Scienze della Terra, Università di Pavia, via Ferrata 1, 27100 Pavia, Italy
[2]Department of Earth Sciences, University of Cambridge, Downing Street, Cambridge CB2 3EQ, U.K.
[3]Centro di studio per la Cristallografia e la Cristallochimica, via Ferrata 1, 27100 Pavia, Italy

ABSTRACT

Infrared spectra of ordered (*P2/n*) and disordered (*C2/c*) pyroxenes belonging to the join augite-jadeite were investigated at room temperature in the range 70–1400 cm^{-1}. The spectra change as a function of composition and the phase transition $P2/n \rightarrow C2/c$ produces an increase in band widths. The autocorrelation function quantified changes in line widths due to these effects. Phonons at low frequencies are very sensitive to both changes in composition and degree of order and are indicative of a non-ideal mixing behavior for the *C2/c* solid solution. Phonons at high frequencies depend on the average composition of the samples and not on local configurational changes related to the order-disorder transition. High degrees of local heterogeneity were suggested by the Δ_{corr} values of the *C2/c* omphacites at intermediate compositions. This effect is most evident in the low frequency region of the spectra, corresponding to modes involving, primarily, the M cations. The changes in frequency due to ordering, $\Delta\omega$, and the change in line widths $\delta(\Delta_{corr})_{100-200}$ for the spectral region 100–200 cm^{-1} and $\delta(\Delta_{corr})_{210-800}$ for the range 210–800 cm^{-1} have been used to characterize the state of local order at different compositions. The spectra yield information related to the local structural states of augite-jadeite pyroxenes, down to a unit-cell length scale, which may then be compared with the average structure determined by X-ray diffraction studies of the same samples.

INTRODUCTION

Advances in the quantitative analysis of structural phase transitions have been made using hard mode infrared spectroscopy (HMIRS) (Bismayer 1990; Burns et al. 1996; Harris et al. 1989; Salje et al. 1989, 1992; Salje 1992, 1994; Zhang et al. 1996). A distinctive feature of this approach is that it permits the resolution of structural distortions and local ordering down to an unit-cell length scale. Small changes in frequency ($\Delta\omega$), line width ($\Delta\Gamma$), and intensity (ΔI) of phonon signals correlate closely with the thermodynamic order parameter. The microscopic properties of several pyroxenes belonging to the join augite-jadeite are presented here and compared with the macroscopic behavior of the same samples obtained by X-ray diffraction study as described in part I (Boffa Ballaran et al. 1998). Frequency shifts and variations in line widths were analyzed as a function of composition and degree of order. The autocorrelation function was used as a simple statistical tool to quantify variations of the line widths of phonon bands, to extract information from those parts of the spectra that are too complex for a conventional fitting procedure. We show how the resulting data prove the sensitivity of HMIRS to cation ordering in omphacites and provide new insights into the microscopic mixing behavior of these minerals. A preliminary account of the experimental results presented here has been given by Boffa Ballaran et al. (1997).

EXPERIMENTAL METHOD

Samples are described in part I of this series. Pellets were prepared with extreme care according to a systematic methodology developed in our laboratory over many years. For different minerals, variable grinding conditions and dilutions in CsI, polyethylene, or KBr were tested to determine their ability to obtain reproducible spectra. For pyroxenes ball mill grinding has been found to be too severe, and the samples described here were therefore ground by hand for a measured time (15 min). Identical conditions of mixing the powdered sample and matrix to obtain a high degree of homogeneity, and of pressing sequences to obtain a constant pellet thickness, were followed. Two types of pellets for each sample were prepared under vacuum and used for the different frequency regions. Pellets of polyethylene, weighing 100 mg each and containing 2% of sample were used for the spectral region 70–500 cm^{-1}, whereas pellets of CsI, weighing

* Present address: Department of Earth Sciences, University of Cambridge, Downing Street, Cambridge CB2 3EQ, U.K. E-mail: tiziana@esc.cam.ac.uk

0003–004X/98/0506–0434$05.00

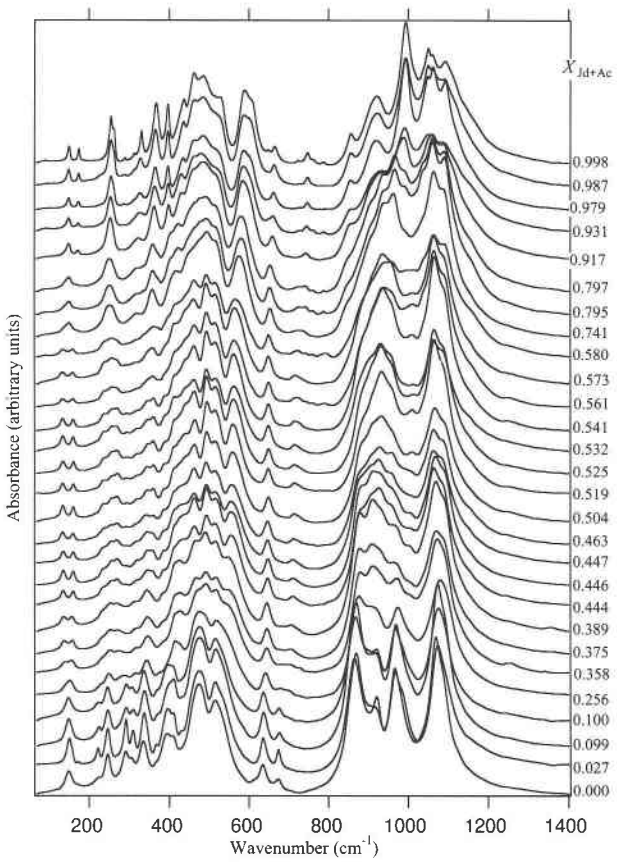

FIGURE 1. Infrared powder-absorption spectra of natural pyroxenes measured at room temperature. A linear base line between 50 and 1400 cm^{-1} has been subtracted. Composition is expressed in this figure and in all the subsequent figures as mole fraction of jadeite + acmite components X_{Jd+Ac}. The third significant figure is shown for X_{Jd+Ac} to spread samples with similar compositions out.

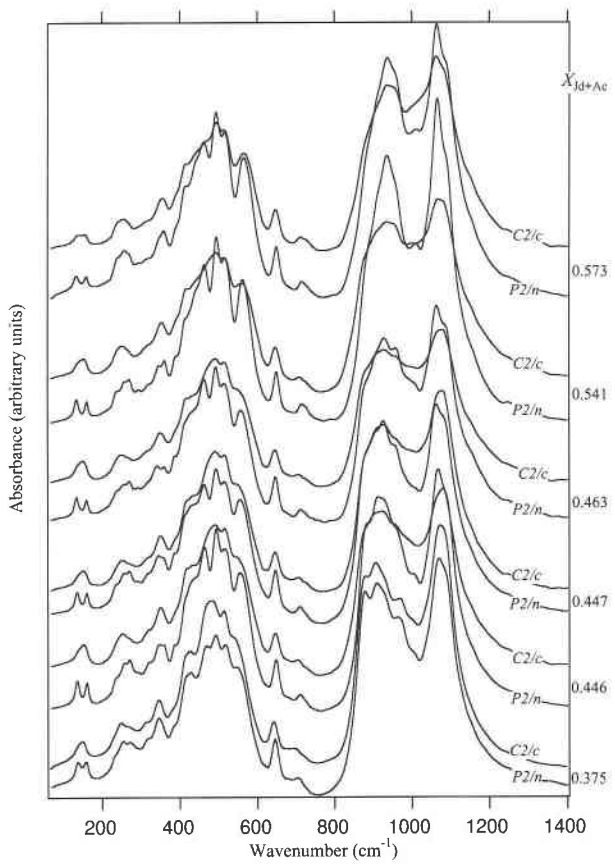

FIGURE 2. Infrared powder-absorption spectra of natural ordered and experimentally disordered omphacites of the same composition measured at room temperature. Changes in the frequency region 100–200 cm^{-1} are immediately apparent.

300 mg each and containing 0.29% of sample were used for the regions 200–700 cm^{-1} and 500–1400 cm^{-1}. Two pellets, one of pure polyethylene (100 mg) and one of pure CsI (300 mg), were prepared following the same conditions and were used as references. To remove absorbed water from the surface of the CsI pellets, they were kept in a oven for 24 h at ~110 °C before collecting the spectra. Spectra were collected under vacuum at room temperature using a Bruker 113V FT-IR spectrometer. A liquid nitrogen-cooled MCT detector for mid-infrared (MIR) and a room-temperature DTGS detector for far-infrared (FIR) were used. Every spectrum was calculated by Fourier transformation of 512 interferometer scans and was recorded as absorbance α, with $\alpha = -\log_{10}(I_{sample}/I_{reference})$, where I is the single-beam transmission intensity. A nominal instrumental resolution of 2 cm^{-1} was used.

INFRARED ABSORPTION SPECTRA

The polyethylene spectra and the CsI spectra were merged by matching up the FIR and MIR sections in the region ~200–400 cm^{-1} where they overlap. The resulting complete series of infrared powder-absorption spectra for natural pyroxenes recorded at room temperature in the region 70–1400 cm^{-1} is shown in Figure 1. The spectra show large changes as a function of composition and degree of order.

IR spectra for natural ordered and experimentally disordered samples for six different compositions are shown in Figure 2. The phase transition *P2/n* → *C2/c* produces an increase in band widths and the number of resolved peaks decreases.

To compare the spectra of experimentally disordered pyroxenes with those of *C2/c* natural samples, samples of N16/2 (X_{Jd+Ac} = 0.099) and SL986 (X_{Jd+Ac} = 0.917) were annealed at high temperature and pressure as described in part I. The IR absorption spectra of the annealed samples equilibrated at high temperature were recorded and compared with the spectra of the corresponding natural pyroxenes. No significant change between the spectra before and after the heat treatment was observed, and we conclude that the local structure of the *C2/c* crystals equilibrated at relatively low temperature during cooling in nature remains the same after the annealing experi-

ments. Hereafter we refer simply to *C2/c* samples without distinction between natural and annealed.

The ordered natural omphacite 74AM33 (X_{Jd+Ac} = 0.525) was progressively disordered at high temperature as described in part I, and the IR powder-absorption spectra of natural and annealed samples were recorded (Fig. 3). Changes in line widths and absorbances of the phonon bands can be noted as a function of the local degree of order. In particular, broadening of the two sharp signals in the region 100–200 cm^{-1} with increasing disorder is clearly visible.

Results

Diopside is expected to show 27 IR-active modes as derived by factor group analysis (Rutstein and White 1971; Tomisaka and Iishi 1980). Extra modes are expected in the spectra of the investigated natural samples because of the occurrence of small amount of impurities. Moreover, in the spectra of omphacites the number of phonon signals increases because of the lowering of symmetry due to the cation ordering. As found for many solid solutions, two-mode behavior (Burns et al. 1996; Hofmeister and Chopelas 1991) might be reasonably expected at low frequencies. It is therefore not straightforward to be confident about detailed trends of the observed signals as a function of composition or to make precise assignments of the IR modes. On the other hand, it is known that all IR modes must change in frequency in response to changing degree of order. In other words, changes in frequency of individual absorption peaks, whether or not their symmetry and eigenvectors are known, contain quantitative information about the order parameter. To explore such relationships in the present case of complicated spectra, an empirical procedure has been followed.

The detailed analysis was done on the unmerged spectra. Phonon signals in the regions 100–200 cm^{-1} and 610–800 cm^{-1} were chosen for the line-profile analysis because of their small overlap with other modes. A previous assignment of the IR absorption bands of diopside (Tomisaka and Iishi 1980) ascribes the phonon peaks in the region 100–200 cm^{-1} to translatory lattice modes dominated by the motions of the large cations in the M1 and M2 sites, and the phonon signals in the range between 610 and 800 cm^{-1} to Si-O-Si stretching modes.

Details from the spectral range 100–200 cm^{-1} are shown for the series of natural pyroxenes in Figure 4 and for the disordered *C2/c* samples (natural, experimentally disordered, and synthetic) in Figure 5. The two sharp and well-defined peaks in the spectra of the natural-ordered omphacites (Fig. 4) coincide with a very broad peak in the spectra of the disordered samples with the same composition (Fig. 5). We have taken this to imply that the phonon band at around 150 cm^{-1} in the spectrum of Aug is split into two peaks in the ordered omphacites. Two Lorentzian profile functions were therefore used for the fitting procedure of this signal. In addition one Lorentzian profile was used in the end-member spectra for the signal

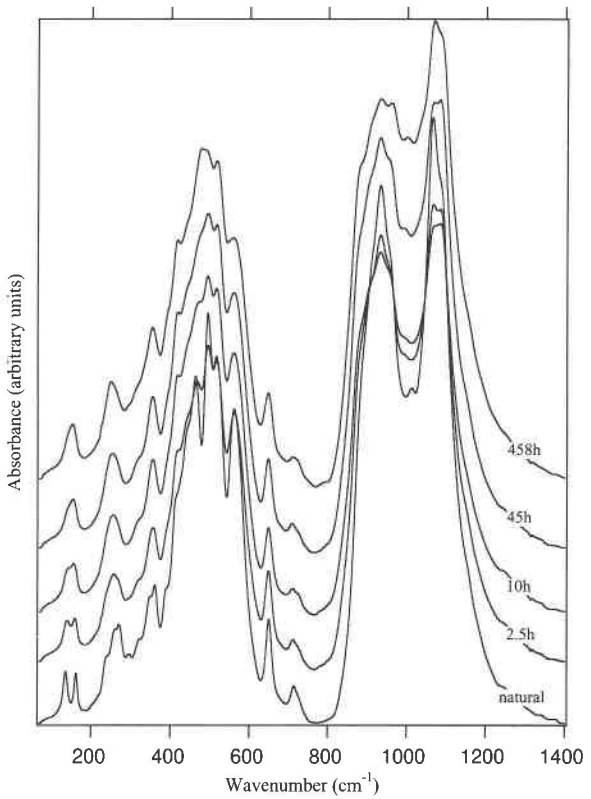

Figure 3. Room-temperature IR powder-absorption spectra of the natural ordered omphacite 74AM33 (X_{Jd+Ac} = 0.525) and of progressively disordered crystals of the same sample annealed at high temperature for 2.5, 10, 45, and 458 h. The disordering process causes clearly visible changes in the phonon line widths and intensities, in particular in the spectral region between 100 and 200 cm^{-1}.

at around 175 cm^{-1} to allow better fitting of the peaks of the range 135–150 cm^{-1}. The resulting peak positions for all the spectra are shown in Figure 6a as a function of composition, expressed as X_{Jd+Ac}. The peak at highest frequencies (crosses) is given only for the samples near the end-members, in that it is not observed at intermediate compositions. The size of the symbols is on the order of the uncertainties. For the other two peaks, the error bars in the figure are approximately an order of magnitude greater than 1σ derived from the fitting procedure. Better results are obtained for the ordered samples whose uncertainties are estimated to be on the order of 0.2–0.4 cm^{-1}. This is a measure of reproducibility using our experimental methodology (see Salje et al. 1989). For disordered samples the uncertainties in the determination of the peak positions are estimated to be on the order of 0.3–0.5 cm^{-1} for the phonon line at higher frequency and on the order of 0.6–0.9 cm^{-1} for the other peak positions at lower frequency that are more scattered. The absolute errors could, of course, be greater, but their magnitudes are not known. Some indication of the real uncertainties is likely to appear as the degree of scatter in the data.

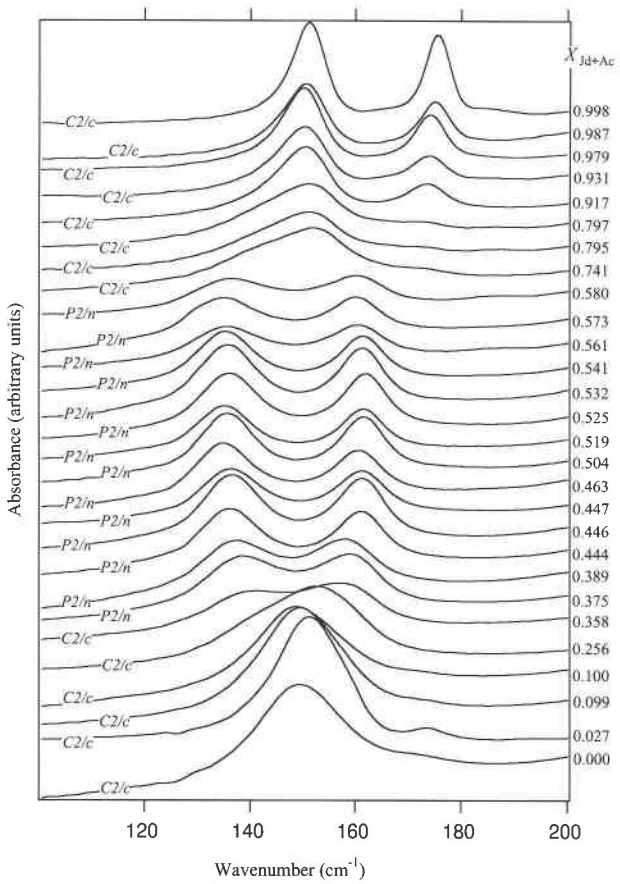

FIGURE 4. Details of the room-temperature IR powder-absorption spectra in the frequency region 100–200 cm^{-1} of natural disordered (*C2/c*) and ordered (*P2/n*) pyroxenes. The signal at around 150 cm^{-1} in the spectra of the end-members is split into two phonon lines in ordered omphacites. Note that the sample at X_{Jd+Ac} = 0.36 has *C2/c* symmetry as determined by X-ray diffraction, but the visible split of the phonon band suggests the presence of short-range order.

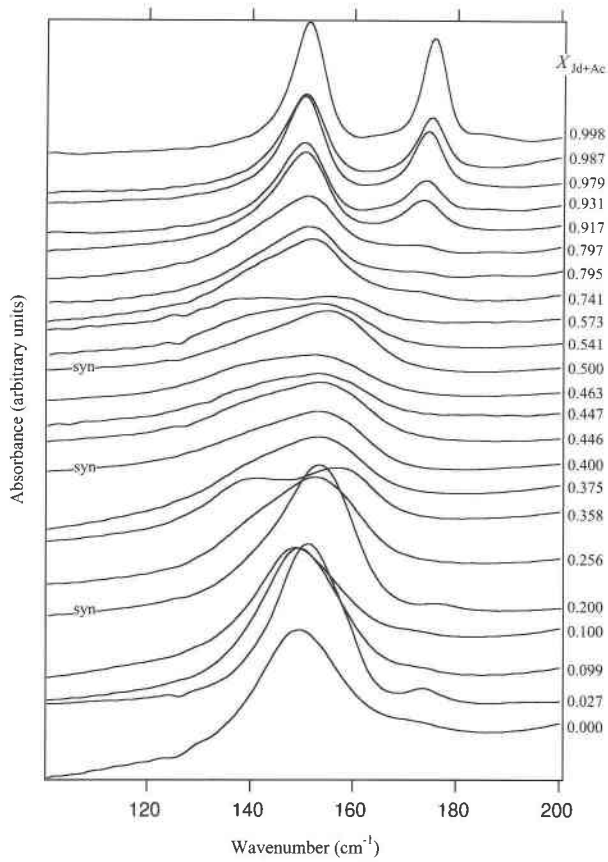

FIGURE 5. Details of the room-temperature IR powder-absorption spectra in the frequency region 100–200 cm^{-1} of *C2/c* samples. Note that disordered omphacites give much broader peaks than the end-member samples. See Figure 4 for note to sample at X_{Jd+Ac} = 0.36.

This empirical procedure leads to the determination of the frequency shifts $\Delta\omega$ between ordered and disordered samples shown in Figure 6a.

Details of the spectra in the region 610–800 cm^{-1} are shown in Figure 7. The relative strong phonon signal at around 635 cm^{-1} shifts as a function of composition and is broader in the spectra of the disordered omphacites (both synthetic and annealed samples). The resulting peak positions of this signal obtained by fitting Lorentzian profiles to its recorded absorption spectrum is given in Figure 8a as a function of composition. Errors in determining peak positions are estimated to be on the order of 0.3–0.5 cm^{-1}.

The relative changes in line width of the absorption profiles were quantified by the autocorrelation function Corr(g,t). This function is defined (Press et al. 1992) as

$$\text{Corr}(g,t) = \int_{-\infty}^{+\infty} g(\tau + t)g(\tau)\, d\tau$$

Corr(g,t) is a function of the lag, t, which is the shift that is applied to the function relative to itself. For small lags the integral is sensitive to the width of the maxima in g, i.e., large values of Corr(g,t) result if the maxima in g are broad, small values result if the maxima are sharp (Malcherek et al. 1995). This procedure has the advantage of giving a statistical measure proportional to the line widths of the phonon lines. Furthermore, it can be used for those regions of the absorption spectra where an analysis achieved by fitting procedures is difficult or impossible because the phonon lines are very broad and overlap each other. Corr(g,t) was calculated for each spectrum after subtracting a linear background from the recorded absorption in four different regions: 100–200 cm^{-1}, 610–800 cm^{-1} (both ranges already used for peak fitting), 210–800 cm^{-1}, and 800–1400 cm^{-1}. Absorption bands in these regions have been ascribed (Omori 1971; Tomisaka and Iishi 1980) at the motions of the M cations and deformations of the pyroxene chains (210–800 cm^{-1}) and to the Si-O stretching modes (800–1400 cm^{-1}). Subsequently Corr(g,t) was scaled to unity at the origin and to zero at a lag of 20 wavenumbers. The halfwidth of the

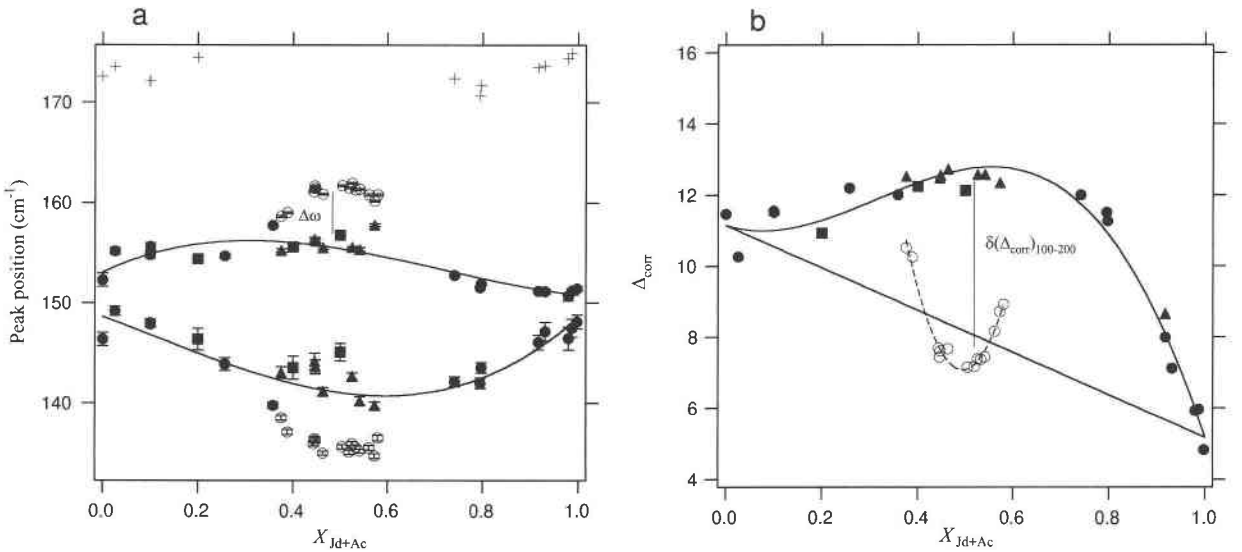

FIGURE 6. (**a**) Peak positions (ω) of the phonon lines in the range 100–200 cm^{-1} as a function of composition. The cross symbols represent the highest frequency peak, observed only in the spectra of the end-members. This may or may not be the same mode in jadeite and augite. For the other two peaks: The curve passing through the lower frequency data is only a guide to the eye to show the pattern of the disordered samples. The curve passing through the data at higher frequencies represents the asymmetric fit of the *C2/c* values using Equation 1 with a_0 = 153.1 ± 0.6, a_1 = −2.3 ± 0.7, a_2 = 24.7 ± 4, and a_3 = 3.0 ± 2. (**b**) Variations of the line widths (Δ_{corr}) measured by means of theautocorrelation function for the same phonon lines as a function of composition. The solid curve represents the asymmetric fit of the *C2/c* data using Equation 2 with b_0 = 11.1 ± 0.4, b_1 = −6.0 ± 0.5, b_2 = 1.8 ± 1, and b_3 = 34.7 ± 2, while the broken curve is only a guide to the eye for the *P2/n* omphacites. Filled circles = *C2/c* samples; open circles = *P2/n* samples; filled triangles = experimentally disordered samples; filled squares = synthetic samples. Note that natural and annealed *C2/c* samples (X_{Jd+Ac} = 0.10 and X_{Jd+Ac} = 0.92) have similar values of Δ_{corr}. $\Delta\omega$ and $\delta(\Delta_{corr})_{100-200}$ are the difference between *C2/c* and *P2/n* values and are proportional to the square of the short-range order parameter q.

resulting function is denoted Δ_{corr} in the following and is proportional to the average of the line widths of the spectral ranges considered. The values of Δ_{corr} for the region 100–200 cm^{-1} are reported as a function of composition in Figure 6b, those for the region 610–800 cm^{-1} in Figure 8b, and those for the other two different regions (210–800 cm^{-1} and 800–1400 cm^{-1}) in Figures 9a and 9b, respectively.

DISCUSSION

It is evident that, for these sodic pyroxenes, changes in the spectra depend on the spectral range examined. The phonon signal at around 150 cm^{-1} is a single band in the spectra of the end-member samples, but is split into two peaks for ordered omphacites (Fig. 4). The separation and the sharpness of the split peaks increases with increasing degree of order. With respect to the *C2/c* solid solution (Fig. 5), however, the same signal for disordered omphacites is much broader than that for the end-members. The sharp peaks of pure augite and jadeite may be interpreted as a result of a homogeneous structure where the only line-broadening influences result from finite temperature and instrumental resolution. Thus, the broadening in line width at intermediate compositions is interpreted as indicative of local heterogeneities in the disordered samples with respect to the end-members, i.e., the structure around each local cation configuration gives a slightly different phonon frequency. Broader line profiles of the *C2/c* samples cannot be ascribed to some consequences of the annealing experiments, because the Δ_{corr} data of the natural and annealed (*C2/c*) N16/2 (X_{Jd+Ac} = 0.099) and SL986 (X_{Jd+Ac} = 0.917) samples have virtually the same values (filled circles and triangles at those two compositions in Fig. 6b).

The values of Δ_{corr} (Fig. 6b) at intermediate compositions for disordered pyroxenes have a positive deviation from ideality, which resembles the positive excess enthalpy of mixing obtained by solution calorimetry (Wood et al. 1980). The values of Δ_{corr} of the *P2/n* phases decreases with increasing degree of order and suggest that the most ordered omphacites, which are colinear with augite and jadeite, are as homogeneous as the end-members. Moreover Δ_{corr} data show an asymmetric behavior not dissimilar from the asymmetric mixing behavior of *C2/c* solid solution described by Holland (1983) and Gasparik (1985). It is possible to fit the *C2/c* peak positions and Δ_{corr} data obtained in the spectral region 100–200 cm^{-1} with asymmetric expressions analogous to the form used for subregular solution models:

$$\omega = a_0 + a_1X_{Jd+Ac} + X_{Jd+Ac}X_{Aug}(a_2X_{Aug} + a_3X_{Jd+Ac}) \quad (1)$$

$$\Delta_{corr} = b_0 + b_1X_{Jd+Ac} + X_{Jd+Ac}X_{Aug}(b_2X_{Aug} + b_3X_{Jd+Ac}) \quad (2)$$

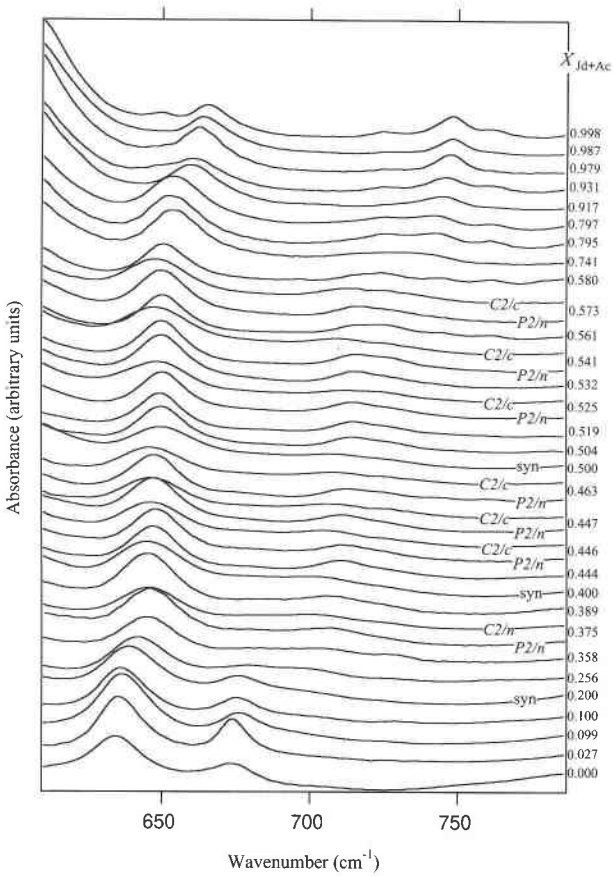

FIGURE 7. Details of the room-temperature IR powder-absorption spectra in the frequency region 600–800 cm^{-1} of the investigated samples. The phonon line at around 635 cm^{-1} in the spectrum of Aug shifts linearly as a function of composition. Disordered omphacites have broader peaks than the corresponding ordered samples.

The difference between peak positions and Δ_{corr} values of *P2/n* samples and the corresponding values, calculated for samples with the same composition but with a disordered structure using Equations 1 and 2, are denoted $\Delta\omega$ and $\delta(\Delta_{corr})_{100-200}$. These parameters have then been used to characterize the state of order of omphacites at different compositions. In general cases, the lowest order dependence of the relevant infrared parameters $\Delta(\omega^2)$, $\Delta\Gamma$, and ΔI on the short-range order parameter q is (Salje 1992, 1994):

$$\Delta(\omega^2),\ \Delta\Gamma,\ \Delta I \propto Aq^2 + Bq^4 \qquad (3)$$

Note that, for small changes in ω, $\Delta(\omega^2) \propto \Delta\omega$.

In the case of omphacites, changes in line width as a function of the local order parameter q are described as $\delta(\Delta_{corr})_{100-200}$ that is, therefore, expected to be linearly dependent on the frequency shift $\Delta\omega$. In Figure 10, the correlation between $\Delta\omega$ and the $\delta(\Delta_{corr})_{100-200}$ is shown. It should be noted that, whereas the natural samples follow the expected linear correlation within experimental uncertainty, the data points of the progressively disordered omphacite 74AM33 deviate from the expected behavior. This correlation between $\Delta\omega$ and $\delta(\Delta_{corr})_{100-200}$ for natural samples, expected from the predicted correlations between changes in line width and frequency for phase transitions, implies that the empirical fitting process used to extract $\Delta\omega$ gives an internally consistent measure of the degree of order in the omphacite samples. For the natural ordered omphacites, at least, we can use both changes in frequency, $\Delta\omega$, and in line widths, $\delta(\Delta_{corr})_{100-200}$, as being indicative of the short-range order parameter q. Finally it should be noted that the scatter in ω values (Fig. 6a) is generally greater than that shown by Δ_{corr} (Fig. 6b), particularly in relation to the total variations with composition and order. This is a reflection of the inherent uncertainties in fitting multiple peaks across a solid solution. Δ_{corr} provides a more reliable, and, probably, more accurate indicator of the ordering and mixing behavior.

Peak positions and Δ_{corr} values in the spectral region 610–800 cm^{-1} (Fig. 8a and 8b) define a different behavior. These phonons are evidently independent of the local configurational changes that accompany ordering or disordering of Ca, Na between the M2 sites, and Mg (Fe^{2+}), Al (Fe^{3+}) between the M1 sites, but they do vary with the average cation content of the samples. The peak position around 635 cm^{-1} in the spectrum of augite (Fig. 8a) shifts linearly with chemical composition and displays a discontinuity around $X_{Jd+Ac} \approx 0.75$. This change in slope coincides with the position of the proposed miscibility gap (Dobretsov et al. 1971; Carpenter 1980, 1983) between ordered omphacite and jadeite. The relative widths of this phonon lines vary only slightly with composition. A positive deviation from ideality of the *C2/c* Δ_{corr} values (less than 2 cm^{-1} for intermediate disordered samples) (Fig. 8b) can still be noted, as well as a small effect due to the ordering. Thus the tetrahedral chains may be thought of as ramrods that are sensitive only to an average composition and that accommodate chemical and order variations with a global distortion that is uniform on both microscopic and macroscopic length scales. With respect to Si-O modes, at least, the local structure appears to remain practically homogeneous over all compositions.

The plot of Δ_{corr} values in Figure 9a and 9b confirms the different behavior of low-frequency and high-frequency phonons. The changes in line widths in the spectral range 210–800 cm^{-1} (Fig. 9a) are sensitive to both changes in composition and degree of order, although the positive deviation from ideality is smaller than for the region 100–200 cm^{-1} (Fig. 6b). Moreover, the pattern of the *P2/n* pyroxenes (broken line) differs from that in Figure 6b for the same samples. If $\delta(\Delta_{corr})_{210-800}$ is scaled in the same way as $\delta(\Delta_{corr})_{100-200}$, a linear correlation between $\delta^2(\Delta_{corr})_{100-200}$ and $\delta(\Delta_{corr})_{210-800}$ (Fig. 11) is found for natural ordered omphacites. This corresponds to the relation (from Eq. 3):

$$\delta(\Delta_{corr})_{100-200} \propto q^2$$

In this case there is a rapid convergence of the expansion 3 with $A \gg B$ so that higher order terms may be ignored.

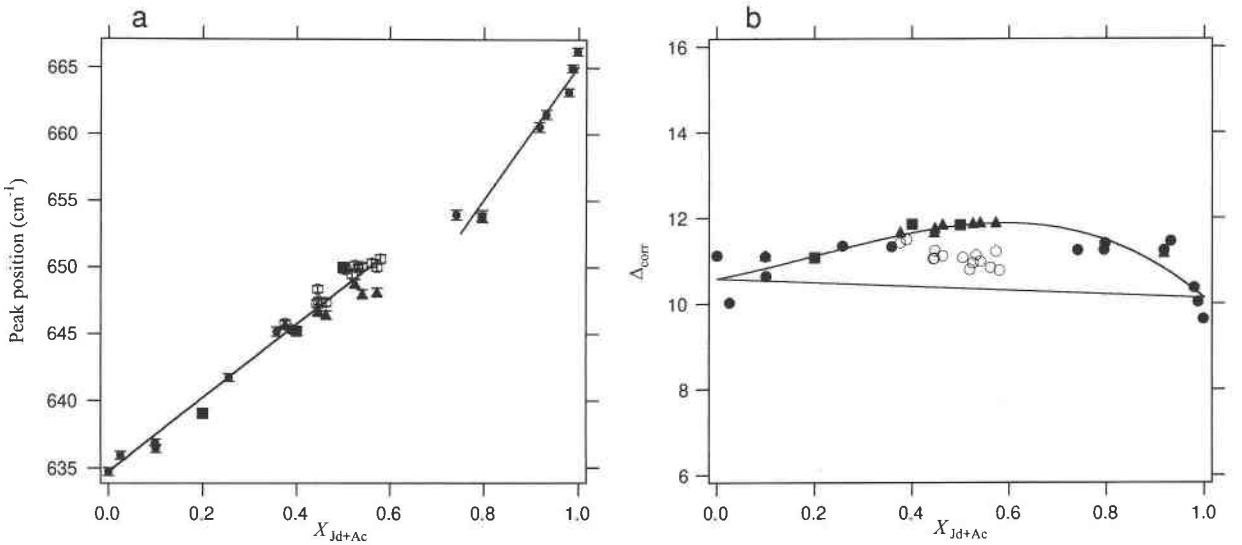

FIGURE 8. (**a**) Frequency shift of the relative strong phonon line at around 650 cm^{-1} (635 cm^{-1} in augite) as a function of composition. Symbols as in Figure 6. The straight lines shown are guides to the eye. The discontinuity obtained from this simple approach coincides with the miscibility gap between ordered omphacite and jadeite. Perhaps there are significant structural differences between jadeite and augite-rich samples, at least with respect to their phonon characteristics. (**b**) Variation of Δ_{corr} values for the range 610–800 cm^{-1} as a function of composition. The *C2/c* Δ_{corr} data show a positive deviation from ideality that is less than 2 cm^{-1} at intermediate composition. The curve shown was obtained by fitting the data with Equation 2 with $b_0 = 10.6 \pm 0.2$, $b_1 = -0.5 \pm 0.2$, $b_2 = 2.5 \pm 1$, and $b_3 = 9.1 \pm 2$. Note a small effect due to the ordering process.

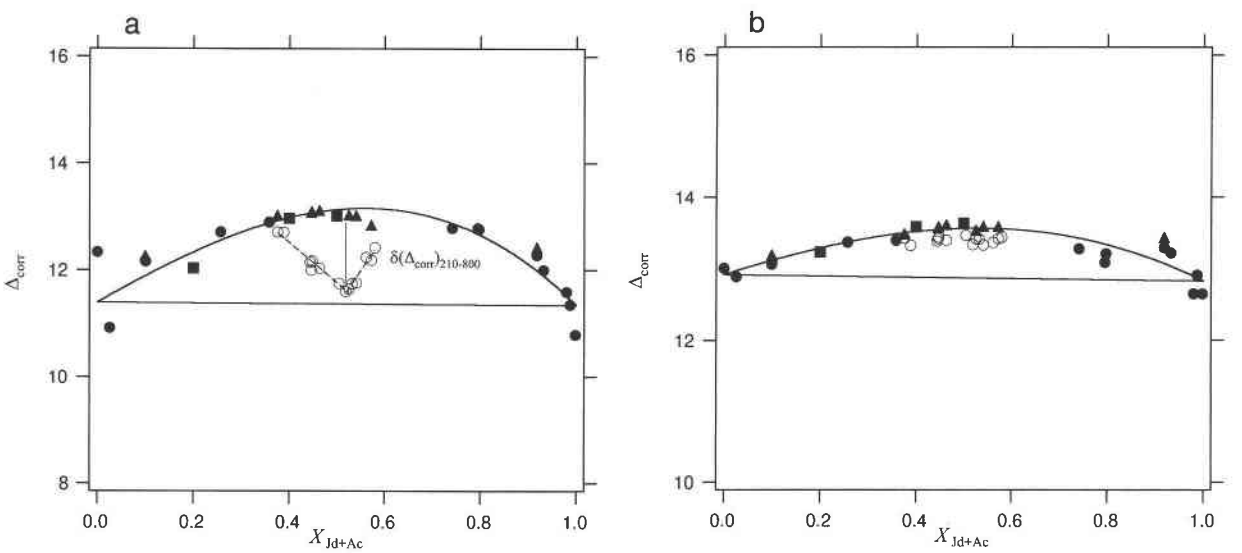

FIGURE 9. (**a**) Variation of Δ_{corr} values as a function of composition in the frequency region 210–800 cm^{-1}. The curve through the *C2/c* data has been obtained from Equation 2 with $b_0 = 11.4 \pm 0.2$, $b_1 = -0.1 \pm 0.2$, $b_2 = 5.2 \pm 2$, and $b_3 = 8.8 \pm 2$. The broken lines are guides to the eye for the *P2/n* omphacites. The difference between ordered and disordered samples is denoted $\delta(\Delta_{corr})_{210-800}$. (**b**) Variation of Δ_{corr} values as a function of composition in the frequency region 800–1400 cm^{-1} related to the Si-O stretching modes. In this frequency range the phonons are insensitive to changes in the degree of order. The positive deviation from ideality of the *C2/c* Δ_{corr} data is smaller than 1 cm^{-1}. Symbols as in Figure 6. Note the different scale for Δ_{corr} for the two different regions.

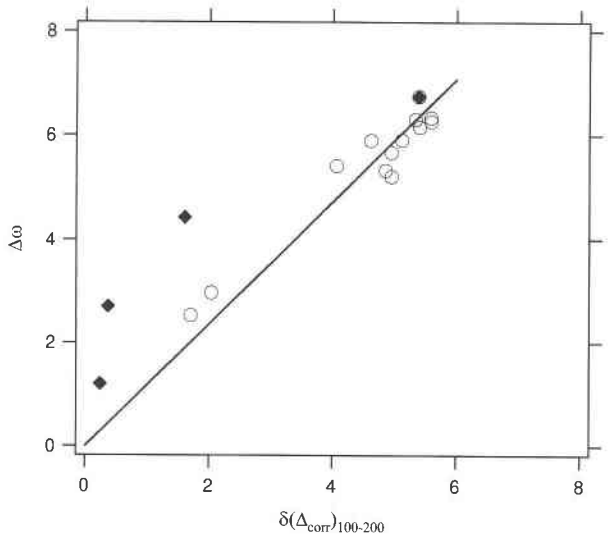

FIGURE 10. Correlation of the change in frequency $\Delta\omega$ between ordered and disordered omphacites with the corresponding change in line widths $\delta(\Delta_{corr})_{100-200}$ calculated in the spectral region 100–200 cm^{-1}. Open circles = natural ordered omphacites; filled diamonds = progressively disordered 74AM33 sample. The straight line shown represents the expected correlation between changes in frequency and line width related to the degree of order. The kinetic data fall significantly off the expected linear trend.

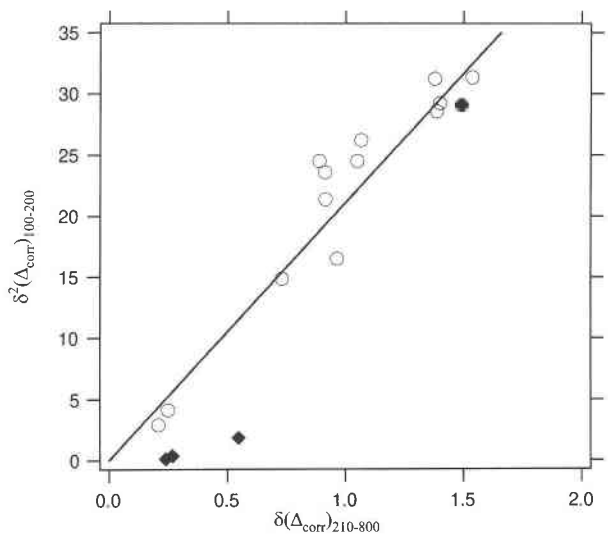

FIGURE 11. Plot of the square of the difference in Δ_{corr} values between disordered and ordered omphacites in the range 100–200 cm^{-1}, $\delta^2(\Delta_{corr})_{100-200}$, against the difference calculated in the same way in the region 210–800 cm^{-1}, $\delta(\Delta_{corr})_{210-800}$. The linear correlation found suggests that $\delta(\Delta_{corr})_{100-200}$ depends on the square of the short-range order parameter q and $\delta(\Delta_{corr})_{210-800}$ depends on q^4. Symbols as in Figure 10.

On the other hand, it follows from Figure 11 that the q^4 term governs the relation between line broadening and short-range order parameter in the region 210–800 cm^{-1}: $\delta(\Delta_{corr})_{210-800} \propto q^4$ i.e., $A = 0$ and $B \neq 0$ in Equation 3, for reasons not yet clear. The correlation of these two parameters of the progressively disordered crystals suggests a different behavior for the non-equilibrium sequence.

Almost no information concerning the different degree of order or compositional heterogeneity can be obtained from the Si-O stretching modes. In fact, in the region 800–1400 cm^{-1} (Fig. 9b), the deviation from ideality at intermediate compositions is negligible (<1 cm^{-1}) and disordered and ordered samples have practically the same Δ_{corr} values.

The main results of the IR analysis may be summarized as follows: (1) The autocorrelation function, which gives a measure proportional to the line widths of the phonon bands clearly provides a useful tool for the quantitative investigation of complex spectra; (2) Synthetic and natural samples behave in the same way, confirming that the low Fe^{+3} contents of the natural pyroxenes investigated only have minor influence on the mixing behavior; (3) Large frequency shifts and variations in line widths occur as functions of both composition and degree of order; (4) Tetrahedral and octahedral chains show a different behavior with respect to changes in composition and degree of order. Si-O modes are practically independent of the local ordering and depend only on the average structure, whereas M-O modes are very sensitive to the local degree of order and suggest a high degree of heterogeneity on a local length scale in disordered crystals of intermediate composition.

MICROSCOPIC VS. MACROSCOPIC BEHAVIOR

New insights into the solid-solution and cation-ordering behavior of the system augite-jadeite may be obtained by comparing the results from the X-ray diffraction study (part I) with the spectroscopic data. With respect to the degrees of order of the investigated samples, the correlation between the square of the long-range order parameters (Q^2_{M1}, Q^2_{M2}) calculated in part I and the square of the short-range order parameter expressed as $\delta(\Delta_{corr})_{100-200}$ in the region 100–200 cm^{-1} is shown in Figures 12a and 12b. Despite the scatter, the data are consistent with a linear correlation between the microscopic and macroscopic order. It is important to note that the frequencies of the analyzed modes are inversely related to the characteristic length scale of the IR measurements (Salje 1992), which may be on the order of four unit cells at such low frequencies. Thus even at a length scale of only a few unit cells, no evidence exists for a more fully ordered local structure. This suggests that the true local structure responsible for the average ¼–¾ ordering in M2 sites occurs at an even shorter length scale. A different behavior is followed by the samples annealed to produce intermediate state of order. Although their long-range order parameters Q_{M1} and Q_{M2} are linearly correlated (Fig. 2 in part I) and are consistent with the expected behavior followed also by the samples equilibrated in nature, a difference on the local configuration between progres-

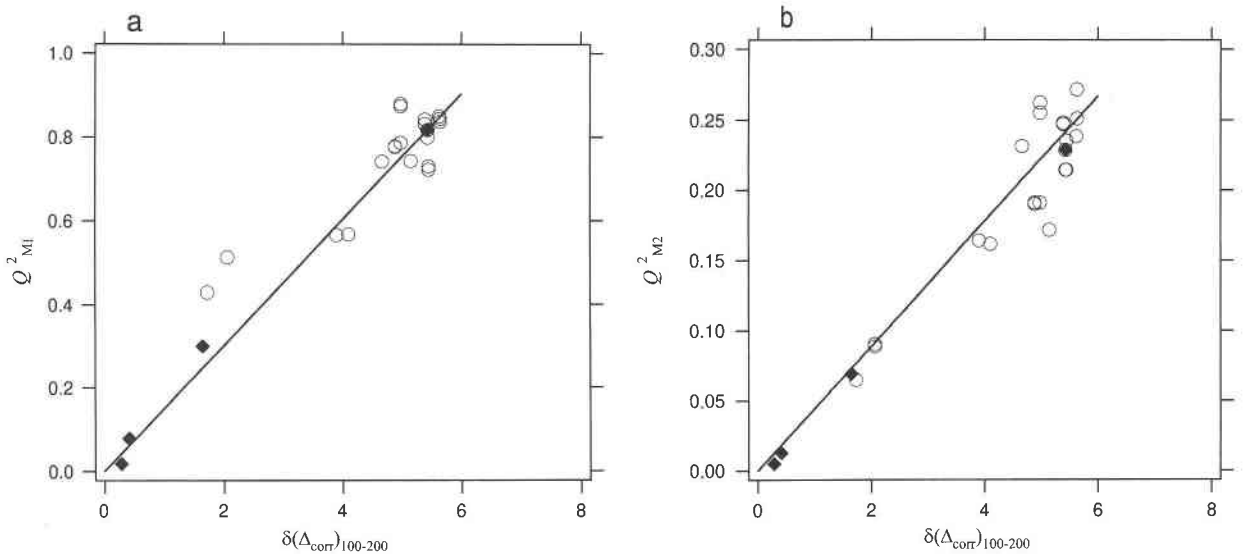

FIGURE 12. Correlation between the square of the long-range order parameters calculated from X-ray single-crystal diffraction data, (**a**) Q^2_{M1} and (**b**) Q^2_{M2} and the squared short-range order parameter expressed as $\delta(\Delta_{corr})_{100-200}$. Symbols as in Figure 10. The scatter of the data is especially due to the uncertainties in the determination of the long-range order parameters (on the order of ±0.01–0.03). The data are, however, consistent with a linear correlation with the short-range order parameter. The straight lines are least squares fits to the data, constrained to pass through the origin.

sively disordered and natural omphacites is observed in the plot of $\Delta\omega$ against $\delta(\Delta_{corr})_{100-200}$ (Fig. 10) and in the plot $\delta^2(\Delta_{corr})_{100-200}$ against $\delta(\Delta_{corr})_{210-800}$ (Fig. 11). The data from the progressively disordered omphacites 74AM33 depart from the expected linear correlation between the two microscopic parameters. The local structure, presumably because of the cation-ordering configuration, is evidently distinct in samples from the non-equilibrium sequence in comparison with the samples that equilibrated in nature.

The behavior of the solid solution strongly depends on the characteristic length scale of the experiments. The unit-cell parameters follow an ideal pattern from pure augite to pure jadeite (Wood et al. 1980; and Figs. 3a and 3b in part I), as do the mean bond distances of tetrahedra and octahedra (Fig. 5 in part I). However, the Δ_{corr} values, calculated for the spectral region related to the low frequency modes, display a highly asymmetric positive deviation from ideality (Fig. 6b). As discussed before, the broadening of absorption bands over the 100–200 cm^{-1} range of the spectra is interpreted in terms of heterogeneities in the local structure around the M1 and M2 cations in disordered omphacites. In particular, the positions of the O2 atoms and, hence, the M-O bond lengths, are sensitive to the precise occupancies of the adjacent cation sites (part I). These microscopic effects correlate with the positive excess enthalpy of mixing shown by the *C2/c* solid solution and are presumably an important factor in the non-ideality. There is also some evidence, comparing the frequency shift analyzed in Figure 8a of the phonon line related to the Si-O-Si stretching modes with the unit-cell volume (Fig. 13), that the structure of jadeite-rich

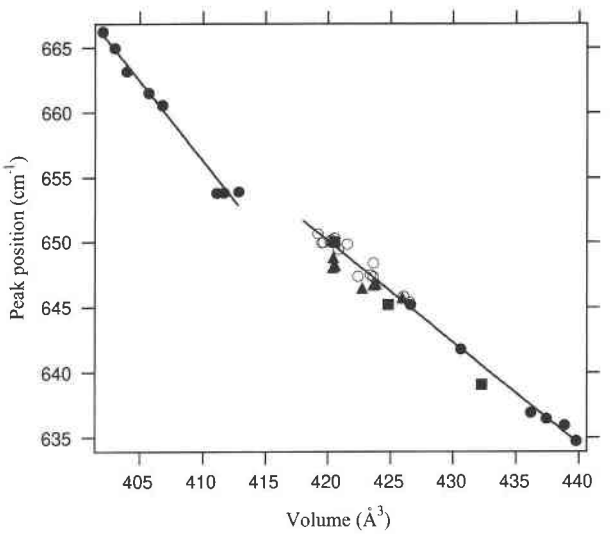

FIGURE 13. Unit-cell volume dependence of the phonon frequencies related to the Si-O-Si stretching modes (610–800 cm^{-1}). Symbols as in Figure 6. The two straight lines were obtained by linear fits of the jadeite-rich pyroxenes data [ω = 1158(±26) − 1.22(±0.06)V] and of omphacites and augite-rich samples data [ω = 978(±15) − 0.078(±0.04)V]. The discontinuity around 75% Jd is consistent with the change in slope observed for the frequency shift of the same peak position as a function of composition and may reflect some significant structural difference between jadeite-rich and augite-rich pyroxenes.

samples is subtly different from that of augite-omphacite crystals. An apparent discontinuity in Figure 13 coincides with the miscibility gap between jadeite and ordered omphacite.

All the microscopic strains related to the cation ordering and substitution in the system Aug-Jd are, however, accommodated by the global distortion of the tetrahedral chains, which are rigid along their lengths but whose tetrahedra are relatively free to move in directions perpendicular to the chains.

Acknowledgments

The authors thank R. Bocchio, R. Compagnoni, T. Holland, B. Lombardo, C. Malgarotto and R. Tribuzio for supplying most of the pyroxenes samples. We also thank M. Zhang for his helpful advises during the experimental work, and B. Kolesov and W. White for reviews of the manuscript. Financial support was provided by MURST (grant 40% V. Tazzoli).

References cited

Bismayer, U. (1990) Hard mode Raman spectroscopy and its application to ferroelastic and ferroelectric phase transitions. Phase Transitions, 27, 211–267.

Boffa Ballaran, T., Carpenter, M.A., Domeneghetti, M.C., and Tazzoli, V. (1997) Hard mode infrared spectroscopy of cation ordering and substitution in a chain silicate. Phase Transitions, 63, 159–170.

——— (1998) Structural mechanisms of solid solution and cation ordering in augite-jadeite pyroxenes I: A macroscopic perspective. American Mineralogist, 83, 419–433.

Burns, P.C., Hawthorne, F.C., Hofmeister, A.M., and Moret, S.L. (1996) A structural phase–transition in $K(Mg_{1-x}Cu_x)F_3$ perovskite. Physics and Chemistry of Minerals, 23, 141–150.

Carpenter, M.A. (1980) Mechanisms of exsolution in sodic pyroxenes. Contributions to Mineralogy and Petrology, 71, 289–300.

———(1983) Microstructures in sodic pyroxenes: implications and applications. Periodico di Mineralogia—Roma, 52, 271–301.

Dobretsov, N.L., Lavrebt'yev, Y.G., and Pospelova, L.N. (1971) Immiscibility in Na-Ca pyroxenes. Doklady Akademii Nauk SSSR, 201, 152–155.

Gasparik, T. (1985) Experimentally determined compositions of diopside-jadeite pyroxene in equilibrium with albite and quartz at 1200–1350°C and 15–34 kbar. Geochimica et Cosmochimica Acta, 49, 865–870.

Harris, M.J., Salje, E.K.H., Güttler, B.K., and Carpenter, M.A. (1989) Structural states of natural potassium feldspar: An infrared spectroscopic study. Physics and Chemistry of Minerals, 16, 649–658.

Hofmeister, A.M. and Chopelas, A. (1991) Vibrational spectroscopy of end-member silicate garnets. Physics and Chemistry of Minerals, 17, 503–526.

Holland, T.J.B. (1983) The experimental determination of activities in disordered and short-range ordered jadeitic pyroxenes. Contributions to Mineralogy and Petrology, 82, 214–220.

Malcherek, T., Kroll, H., Schleiter, M., and Salje, E.K.H. (1995) The kinetics of the monoclinic to monoclinic phase transition in $BaAl_2Ge_2O_8$-feldspar. Phase Transitions, 55, 199–215.

Omori, K. (1971) Analysis of the infrared absorption spectrum of diopside. American Mineralogist, 56, 1607–1616.

Press, W.H., Teukolsky, S.A., Vetterlin, V.T., and Flannery, B.P. (1992) Numerical recepies in FORTRAN, p. 492. Cambridge University Press, Cambridge.

Rutstein, M.S. and White, W.B. (1971) Vibrational spectra of high-calcium pyroxenes and pyroxenoids. American Mineralogist, 56, 877–887.

Salje, E.K.H. (1992) Hard mode spectroscopy: Experimental studies of structural phase transitions. Phase Transitions, 37, 83–110.

———(1994) Phase transitions and vibrational spectroscopy infeldspars. In I. Parson, Ed., Feldspars and their Reactions, p. 103–160. Kluver, Dordrecht, the Netherlands.

Salje, E.K.H., Güttler, B., and Ormerod, C. (1989) Determination of the degree of Al,Si order Q_{od} in kinetically disordered albite using hard mode infrared spectroscopy. Physics and Chemistry of Minerals, 16, 576–581.

Salje, E.K.H., Ridgewell, A., Güttler, B. Wruck, B., Dove, M.T., and Dolino, G. (1992) On the displacive character of the phase transition in quartz: a hard mode spectroscopy study. Journal of Physics C Condensed Matter, 4, 571–577.

Tomisaka, T. and Iishi, K. (1980) Some aspect of the lattice dynamics of diopside. Mineralogical Journal, 10, 84–96.

Wood, B.J., Holland, T.J.B., Newton, R.C., and Kleppa, O.J. (1980) Termochemistry of jadeite-diopside pyroxenes. Geochimica et Cosmochimica Acta, 44, 1363–1371.

Zhang, M., Wruck, B., Graeme Barber, A., Salje, E.K.H., and Carpenter, M.A. (1996) Phonon spectra of alkali feldspars: Phase transitions and solid solutions. American Mineralogist, 81, 92–104.

Manuscript received February 12, 1997
Manuscript accepted December 24, 1997
Paper handled by George A. Lager